Available online at www.sciencedirect.com

ScienceDirect

Soils and Foundations 60 (2020) 167–178

www.elsevier.com/locate/sandf

Technical Paper

Contact erosional behaviour of foundation of pavement embankment constructed with nanosilica-treated dispersive soils

Amir Hossein Vakili [a,b,*], Seyyed Iman Shojaei [c], Mahdi Salimi [d], Mohamad Razip bin Selamat [e], Mohammad Sadegh Farhadi [f]

[a] Department of Civil Engineering, Faculty of Engineering, Zand Institute of Higher Education, Shiraz, Iran
[b] Young Researcher and Elite Club, Estahban Branch, Islamic Azad University, Estahban, Iran
[c] Department of Civil Engineering, Estahban Branch, Islamic Azad University, Estahban, Iran
[d] Faculty of Engineering, Hamedan Branch, Islamic Azad University, Hamedan, Iran
[e] School of Civil Engineering, Universiti Sains Malaysia, 14300 Nibong Tebal, Penang, Malaysia
[f] Faculty of Built Environment, Tampere University, Tampere, Finland

Received 15 April 2019; received in revised form 22 January 2020; accepted 16 February 2020
Available online 3 March 2020

Abstract

To overcome the problems associated with the construction of pavement layers on soft subgrade, working platforms constructed with granular soils are normally placed beneath the overlying paving layers. Sometimes, the embankment layer located between the pavement and the working platform layers may have dispersive nature. In such case, the dispersive soil particles can be easily transported through the large pores of the working platform layer under water movement, resulting in soil loss of the dispersive embankment and the subsequent settlement of the pavement layers. In other words, dispersive soils are susceptible to contact erosion. Therefore, the contact erosional behaviour of the dispersive embankment layer placed on granular materials must be investigated. In the current study, the contact erosion of both the dispersive embankment and also the nanosilica-treated dispersive embankment cured for periods of up to 28 days was investigated experimentally under the vertical flow of groundwater. The significant mass loss was measured when the embankment layer was highly dispersive. However, the mass loss decreased by treating the dispersive embankment layer using an environmentally friendly stabilizer named nanosilica, which reflected the high potential use of the nanosilica to improve the dispersive soils. Besides, it was verified by the Scanning Electron Microscope (SEM) and Fourier Transform Infrared (FTIR) spectra tests on the natural dispersive soil samples and the ones after being treated by nanosilica. The plasticity index decreased and unconfined compressive strength increased due to addition of nanosilica to the dispersive soil; thus, its workability improved. The dispersion and contact erosion tests results indicated that there was a very good correlation between dispersivity potential and some contact erosion assessment parameters, such as void ratio, collected eroded soil and settlement. In conclusion, the contact erosion rate can be estimated based on the relationships proposed in this study.

Keywords: Contact erosion; Dispersive soil treatment; Nanosilica; Pavement embankment's foundation; Settlement

1. Introduction

Dispersive soils are prone to the internal erosion failure. One of the subclasses of the internal erosion is named as contact erosion, in which the particles of the soil layer with finer grains are moved into the coarse-grained layer pores along with the water flow. In other words, contact erosion occurs at the interface of two embankment layers with different sizes of particles (Beguin et al., 2012b). As shown in Fig. 1, this mechanism occurs where a coarse-grained soil is in contact with a fine-grained material, and water flow erodes the fine soil toward the contact surface with the

Peer review under responsibility of The Japanese Geotechnical Society.
* Corresponding author.
E-mail addresses: a.vakili@zand.ac.ir (A.H. Vakili), cemrs@eng.usm.my (M.R.b. Selamat).

https://doi.org/10.1016/j.sandf.2020.02.001
0038-0806/© 2020 Production and hosting by Elsevier B.V. on behalf of The Japanese Geotechnical Society.

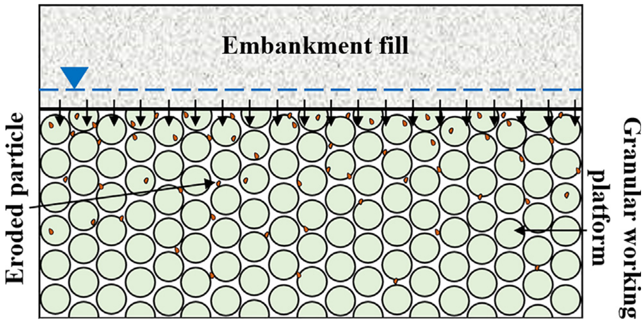

Fig. 1. Mechanism of contact erosion due to change of ground water level (Premkumar, 2017).

coarse soil. The main turbulent flows that can affect the in-service granular material are air turbulence from moving vehicles in a roadway and water runoff. A concentrated flow, such as water runoff, is energetic and has the necessary energy to drag soil particles (Bilodeau et al., 2007). The loss of finer particles encountered on the shoulder of unpaved or paved roads due to the turbulent flows is a problem of great concern. Furthermore, heavy vehicles circulating on roads deteriorate the stability and erosion problem. Generally, the particles dragged from the soil matrix are mostly silt and clay particles due to their light weight. The differential settlements, normally occurred in the road embankments, are an outcome of the temporal progression of the cavities that are resulted from the contact erosion phenomenon (Jegatheesan et al., 2015).

Many of previous studies have reported road failure caused by such erosion. Migration of fine particles in pavement may also remarkably decrease the period between necessary maintenance (Trani and Indraratna, 2010). The presence of the void beneath the pavement slab leads to an increase in stress and strain in the pavement and finally may result in other failures such as pavement cracking (Huang, 2004). de OS and Carlos (1991) stated that water from rainfall enters the cracks during the wet season and leads to internal erosion along deep cracks. Different settlements along longitudinal cracks as well as collapsed holes can arise from climatic cycles, traffic loadings and internal erosion (i.e., backward erosion, contact erosion, concentrated leak erosion, and suffusion). It should be noted that the moisture of the pavement structure has a large effect on its efficiency (Premkumar, 2017). Such that excess moisture in the pavement can cause a failure in the pavement structure (Schaefer et al., 2008). Increasing the water level with minimum mechanical effect on the embankment made of dispersive clays can initiate contact erosion failure. The eroded soils can be transported even in the absence of water flow into the working platform layer due to large pore openings. Consequently, such a situation is well suited to initiate the contact erosion failure at the interface of the embankment fill containing dispersive clays and the granular working platform materials (Premkumar, 2017). After all, the dispersibility of the clay particles and their impact on the failure of contact erosion should be evaluated in detail in order to develop a suitable technique to prevent mass loss. Therefore, geotechnical investigations on road embankments are strongly required to examine their contact erosion potential and the subsequent settlements, and to select the necessary precautions.

To overcome the problems associated with the construction of pavement layers on soft subgrade, working platforms constructed with granular soils are normally placed beneath the overlying road layers and just over the soft subgrade layer (Kazmee et al., 2016). Sometimes, the embankment layer between the pavement and working platform layers may have dispersive nature (Premkumar et al., 2014). In this case, the dispersive materials can be easily transported through the large pores of the working platform layer under water movement and result in the dispersive soil loss and the subsequent settlement of the pavement layers (Premkumar et al., 2015). Thus, the existence of the dispersive soil layer in road embankment may accelerate the contact erosion. Therefore, the contact erosional behaviour of the dispersive embankment located on granular materials is needed to be investigated. In fine-grained soils, dispersive clays are more sensitive when they are exposed to water (Goodarzi and Salimi, 2015a; Vakili et al., 2018b, 2013), and it results in a higher rate of contact erosion. Increasing the water content of these soils can change their mechanical properties and cause soil erosion (Vakili et al., 2015b). Dispersive clays are widely distributed in many parts of the world (Shoghi et al., 2013; Vakili et al., 2018a), so in some areas, the construction of roads on pavement embankment fill with dispersive soil is inevitable (Premkumar et al., 2015). Hence, accurate evaluation of contact erosional behavior of these types of soils in road embankment is necessary to avoid its destructive effects.

In the pavement embankment containing dispersive clays, chemical stabilization can be considered as a solution to overcome the contact erosion failure and to reduce the dispersivity of soil (Goodarzi and Salimi, 2015; Vakili et al., 2017). Many studies have been conducted on the treatment of dispersive soils using chemical stabilizers (Consoli et al., 2016; Savaş et al., 2018; Vakili et al., 2018). Recently, due to its relatively low cost, heat resistance, and environmental compatibility, nanosilica has been considered as a soil stabilizer (Bahmani et al., 2016; Lv et al., 2018). It has been reported the use of nanosilica can play an important role in improving the geomechanical properties of soil. However, its influence on the contact erosional behavior of dispersive soils is needed to be evaluated, especially in the areas where construction projects are executed regardless of whether the soil needs to be stabilized or not.

To date, the contact erosion beneath the embankment dams and dikes has been investigated (Cyril et al., 2009), while the contact erosion of road embankment has been less targeted in research. Hence, in this experimental study, an upward water flow to the pavement embankment was applied in order to assess the contact erosion. In contrast, in dams and dikes, the direction of water flow is usually parallel to the interface between coarse- and fine-grained layers (Beguin et al., 2012b; Cyril et al., 2009). Recently, a new laboratory test method has been introduced to assess the contact erosion of the road embankment layers. In this test method, proposed by Premkumar et al. (2015) and Jegatheesan et al. (2015), mass loss, void ratio, and settlement of the road embankments are the parameters that can be measured in the contact erosion test. Despite the time-consuming and costly testing, it is necessary to predict the contact erosional behavior of soil.

The literature review evidenced the lack of the experimental studies on the contact erosion at the interface between dispersive embankment and granular working platforms, especially, the embankments of nanosilica-treated dispersive soil. Therefore, the main objective of the current study, among others, was to investigate the contact erosional behavior of nanosilica-treated dispersive embankment located on granular working platforms. In addition, the time-consuming and relatively expensive contact erosion tests motivated the researchers to find the correlations between some contact erosion factors, like void ratio, collected eroded soil, and settlement, and the dispersive embankment characteristic feature, i.e. dispersion percentage. It resulted in a relatively accurate prediction of contact erosion factors by measuring the soil dispersivity. A laboratory apparatus, developed by Premkumar et al. (2015) and modified by Jegatheesan et al. (2015), was used to perform the experiments, model the contact erosion, and determine the risk of pavement deformation, while the probable failure due to vertical groundwater flow could be considered (Vakili et al., 2016). The effect of different amounts of nanosilica on the contact erosional behavior of dispersive soils was investigated for different curing periods of 1, 7, 14 and 28 days. In addition, double hydrometer, pinhole, unconfined compressive strength, Atterberg limits, scanning electron microscope, and Fourier Transform Infrared (FTIR) spectra tests were conducted on the dispersive soil and nanosilica-stabilized soil samples.

2. Materials and methods

2.1. Materials

In this study, two types of soils were used to conduct the contact erosion tests, including coarse- and fine-grained soils. The coarse-grained soil was placed in the lower part of the testing apparatus as the working platform material, which was collected from the central district of Shiraz county, Iran. The working platform material provided for the study was classified as poorly graded gravel (GP) based on the Unified Soil Classification System (USCS) and A-1 as per AASHTO soil classification with uniformity and curvature coefficients of 1.5 and 0.937, respectively. It should be noted that the gradation of aggregates meets the requirements of the working platform according to the road and pavement standards of Iran. The maximum and minimum dry densities of the working platform material were measured according to ASTM D 4253-14 and D 4254-14, equal to 1.47 and 1.29 g/cm^3, respectively. In the experiments, the relative density of the working platform material was considered 72% and the dry density was 1.42 g/cm^3. The main function of the working platform, unlike filters used in the embankment dam, is not the erosion control (Premkumar et al., 2015). In other words, the filter criteria cannot be used for granular working platform materials as proposed by Premkumar (2017). Hence, the filtration properties are not appropriate for the working platform materials. Therefore, in accordance with the previous research (Jegatheesan et al., 2015; Premkumar et al., 2015, 2014), it was planned to use coarse-grained layers of 100% passing through a 26-mm sieve.

The fine-grained soil samples used in the experiments were the laboratory dispersed soil samples selected from the small brick making factories zone of Kooshk, in the vicinity of Shiraz, Iran. In order to determine the dispersibility of the samples, double hydrometer and pinhole tests were performed according to ASTM D 4221-11 and D 4647-13, respectively. In addition, the fine-grained soil samples provided for the study were subjected to particle size distribution test according to ASTM D 422-07, Atterberg limits tests according to ASTM D 4318-10, standard laboratory compaction test according to ASTM D 698-12, unconfined compressive strength test according to ASTM D 2166-16, and contact erosion test by following the method described by Premkumar et al. (2015). The physical, chemical, and mechanical properties of the dispersive soil samples are shown in Table 1, and the chemical composition of the dispersive clay sample determined from the X-ray fluorescence (XRF) test is given in Table 2. Fig. 2 presents the grain-size distribution curves of both studied soils. The need for research in the field of nanotechnology and its applications has grown dramatically over the past few decades, as these materials have high market potential and economic effects (Said et al., 2012). Nanosilica used to stabilize dispersive soil samples was provided from Isatis Nanosilica Company located in Yazd, Iran, and its specifications are presented in Table 3. Silica particles are extracted from crystalline natural sources such as quartz, tridymite, cristobalite containing metallic impurities. Nanosilica is known as a low-cost and improved ecological footprint material, which can be a good alternative to replace the traditional additives. The water used in tests was distilled water with pH of 7.

2.2. Sample preparation and methods

The dispersive clay samples provided for the study were initially subjected to laboratory compaction test by following ASTM D 698-12. After determining the optimum moisture content and maximum dry density of the dispersive clay samples, they were stabilized by various proportions

Table 1
Physical and mechanical properties of the dispersive clay sample.

Soil property	Value
Clay content (%)	31
Silt content (%)	50
Sand content (%)	19
Liquid Limit (%)	43
Plastic Limit (%)	20
Plasticity Index (%)	23
Soil classification	CL
Maximum dry density (g/cm^3)	1.72
Optimum moisture content (%)	17.21
Pinhole classification	D_2
Dispersion percent (%)	66.23
Unconfined compressive strength (kPa)	188.3

Table 2
Chemical compositions of the dispersive clay sample.

Formula	Concentration (%)
Al_2O_3	9.005
SiO_2	39.709
Fe_2O_3	4.899
CaO	17.218
Na_2O	1.657
TiO_2	0.499
K_2O	1.826
MnO	<0.1
P_2O_5	1.233
MgO	4.537
LOI	19.4

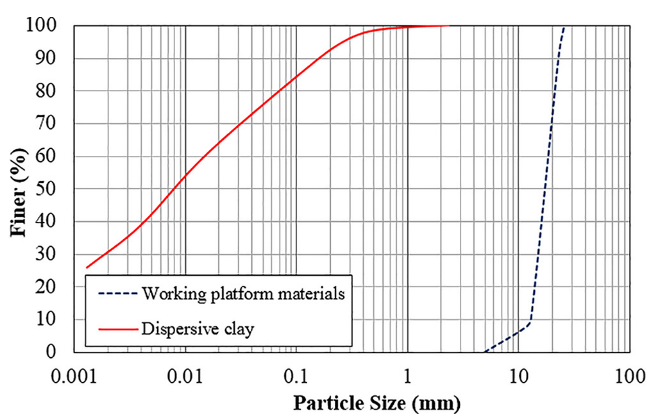

Fig. 2. The grain-size distribution curves of working platform materials and dispersive clay used in this study.

of nanosilica and cured within different periods of time. It should be noted that the specific amount of nanosilica to be added to the dispersive soil samples was first mixed with the distilled water equivalent to the optimum moisture content of the sample, and then the water-additive mixture was thoroughly mixed with soil to obtain uniform soil samples. During the curing process, the prepared soil samples were kept in airtight plastic bags and cured at the ambient room

Table 3
Physical properties of nanosilica.

Property	Value
Molecular Weight (g/mol)	60.08
Purity (%)	>99
Density (g/cm^3)	0.396
Melting point (°C)	1726
Particle size (nm)	15–35
pH	5.7–6.7
Solubility in water (g/lit)	0.15
Shape	Powder
Color	White
Specific surface area, m^2/g	180

temperature, i.e. 25 °C, so that their moisture would not vary. The dispersive clay samples were treated with 0.5, 1, 1.5 and 2% nanosilica, regarding the dry mass of the soil, and in this stage, they were cured for 7 days. Afterwards, the stabilized soil samples were subjected to standard laboratory compaction test and the maximum dry density (MDD) and optimum moisture content (OMC) for each sample were measured, as shown in Fig. 3. Then several other samples were stabilized with the aforementioned nanosilica percentages and cured for 1, 7, 14 and 28 days under their optimum moisture content. The addition of nanoparticles led to an increase in the OMC and a decrease in the MDD of the treated samples. This can be attributed to an immediate formation of cementitious materials such as CSH gel in the presence of nanoparticles reducing compactibility and the density of the nanosilica-treated soil (Bahmani et al., 2014). Besides, the addition of nanosilica to the samples results in the agglomeration and flocculation of the soil particles and the formation of macro-pores that can be easily filled with water, thereby increasing the optimum moisture content.

Double hydrometer tests were carried out in accordance with ASTM D 4221-05 to determine the dispersivity of the samples stabilized with different percentages of nanosilica (up to 2%) and treated at different periods of time (up to 28 days). Based on the double hydrometer results, soil samples are divided into 3 classes, named highly dispersive with dispersion percentage of more than 50%, moderately dispersive with dispersion percentage of between 30 and

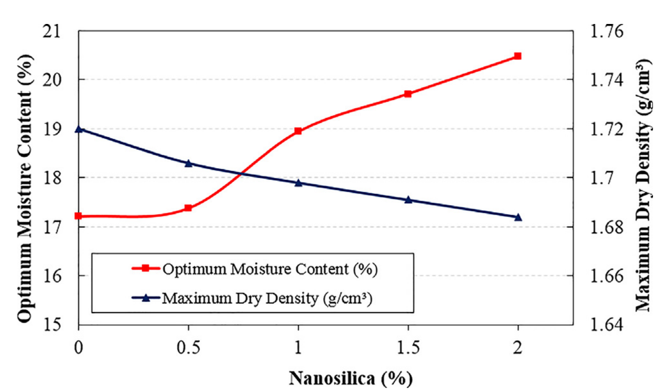

Fig. 3. Values of optimum moisture content and maximum dry density of dispersive soil samples treated by various nanosilica content.

50%, and non-dispersive with dispersion percentage of less than 30%. In general, it is recommended to perform several tests separately to determine the quantitative and qualitative dispersibility of soil accurately (Shoghi et al., 2013). Hence, pinhole test was also performed according to the method A of ASTM D 4647-06 on all samples as a qualitative test method. Based on the pinhole test results, soil samples are categorized into 6 classes. Classes D1 and D2 are dispersive soils, classes ND3 and ND4 are moderately dispersive, and classes ND1 and ND2 are non-dispersive soils. The dispersion percentage of the untreated sample was determined as 66% based on double hydrometer test. In addition, the untreated soil sample provided for the study was classified as D2 based on the pinhole test results. Thus, the fine-grained soil provided for the study was identified as highly dispersive.

The workability, resistance, and permeability of the fine-grained soil could be appropriately estimated by controlling the plasticity of the soil (Vakili et al., 2017). So the plasticity index of nanosilica-treated dispersive clay samples were evaluated by determination of the Atterberg limits. To verify the strength improvement impact, Unconfined Compressive Strength (UCS) tests were performed on the stabilized samples. To prepare the homogeneous specimens for UCS tests, the stabilized soil samples were kept in airtight plastic bags for 24 h. Next, the stabilized samples were compacted inside the UCS mould with 38 mm diameter and 76 mm height in 3 layers with the standard compaction effort. Afterwards, the compacted soil samples were extracted from the mould and cured under their optimum moisture content and maximum dry density in airtight plastic bags for the aforementioned curing time periods. The UCS of the untreated soil samples was 188.3 kPa. In addition, by performing the Scanning Electron Microscope (SEM) and Fourier Transform Infrared (FTIR) spectra tests, the microstructure of dispersive clay samples and nanosilica-treated dispersive clay samples were compared with each other. It is worthy to note that each test was repeated three times to ensure data validity, and the results reported here were the average of the three results.

2.2.1. Contact erosion apparatus

According to ASTM D 2434-06, the cylindrical geometric shape of the main cell with the height, internal diameter, and thickness of 416, 240 and 4 mm, respectively, was selected in order to impose a uniform flow in the samples and to avoid unwanted flow path in the corners. The material of cylinder was transparent acrylic (plexiglass) which causes visibility of the erosion process during the test. Reinforcement bands/strands were used to maximize the cell stability at high pressures. The top and bottom parts of the cylinder were made of steel plate and steel grid, respectively; which were held firmly by six longitudinal screws passed through the edge of the lower steel grid, the reinforcement bands, and also the upper steel plate. Fig. 4 shows the overall view of the contact erosion apparatus used in this study.

The top steel plate was designed movable in order to place materials into the cell. In order to apply a uniform pressure, a circular steel plate of 5 mm thickness and 238 mm in diameter was connected to a loading shaft, vertically moveable through a hole at the centre of the top steel plate. A dial indicator was installed at the end of the loading shaft to measure the vertical deformation. This plate was placed on fine-grained soil and an overload of 1 kPa was applied to prevent swelling and uplift of soil. A conical base was attached beneath the steel grid so that the eroded soil might be removed easily. Besides, a steel mesh was placed on top of the conical base to prevent the accumulation of the working platform particles. The holes size of this mesh was large enough for removal of the eroded soil. Three valves were used in this apparatus. For simulating groundwater at the level of the steel grid, the valve No. 1, at the bottom of the cylinder, was connected to a water inlet tube. The valve No. 2 was a water outlet that was placed below the device, beneath the conical base, to remove the eroded soil. The valve No. 3 was installed in the upper steel plate to discharge air from the cell and remove the air pressure. In addition, a pressure gauge was placed on the top of the apparatus to measure the air pressure inside the cylinder, if necessary. A standpipe was placed before the water inlet valve to indicate the hydraulic head in a sample. To prevent water fluctuations and changes in the pressure of the inlet water as well as to provide water to the device, a water tank was placed at a height from the ground. It should be noted that the apparatus was placed at a height of about 1 m in order to make it easy to drain the water during the test.

2.2.2. Contact erosion tests procedure

The working platform material was compacted in the testing mould in 5 layers and eventually reached the height of 180 mm and relative density of 72%. Dispersive soil was prepared at the optimum moisture content and wrapped in plastic bags for 24 hrs and then kept at the temperature 20 ± 2 °C such that no change in moisture occurred. Then, it was compacted in three layers by 25 drops of a hammer to reach the thickness of 50 mm. Premkumar (2017) evaluated the contact erosion failure for two embankment layer thicknesses of 50 and 150 mm. He found that the cumulative mass of eroded material have a similar trend for both 50 and 150 mm embankment layers. Furthermore, although the amount of the total material eroded for 50 mm embankment fill was lower than that of 150 mm embankment fill, the percentage of material eroded was similar. Hence, in this study, a height of 50 mm was chosen to perform the contact erosion tests because of the similarity of the results in percent. Moreover, it should be noted that in the embankment layer with lower thickness, the difference of applied hydraulic head could also be reduced, resulting in a decrease in the rate of water infiltration into the embankment at the interface, which is the primary initiator of clay dispersion. This

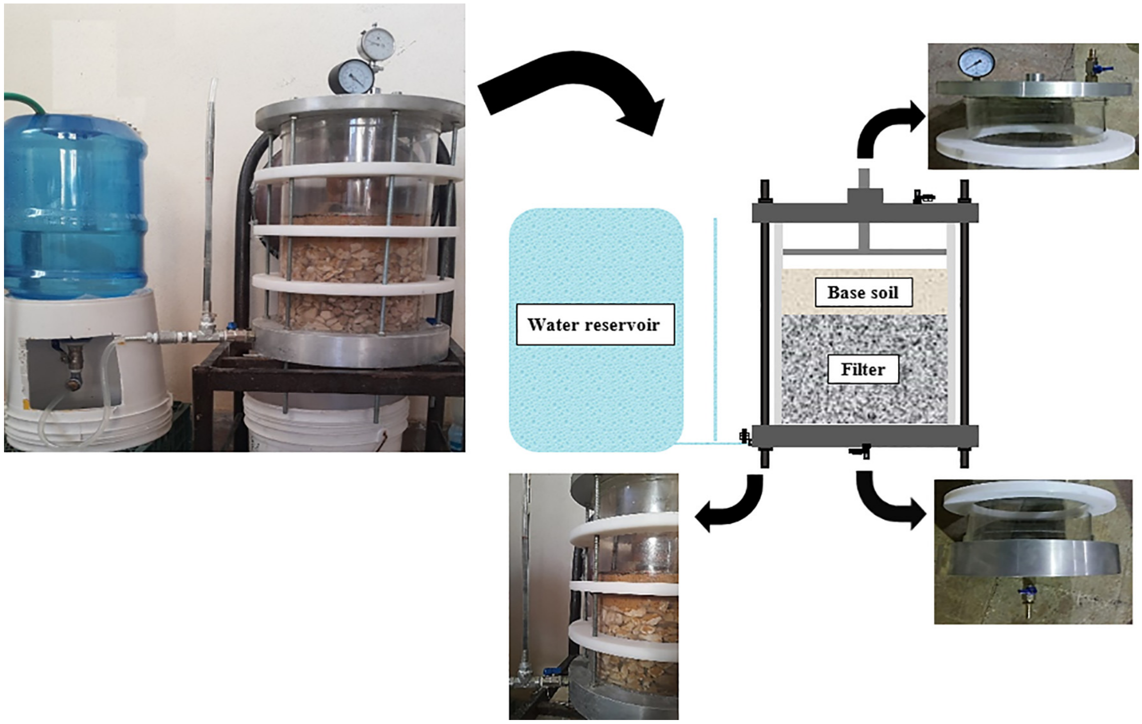

Fig. 4. The overall view of the contact erosion apparatus used in this study.

change in hydraulic head can reduce the mass loss at the interface. In addition, the compaction effect is also considered as an important factor, such that the impact of compaction effort around the interface layer is greater when the embankment fill has a lower thickness.

After assembling the apparatus, in order to simulate the groundwater in soil, the water inlet valve was opened. The water was raised up to the level of 75 mm above the fine-grained soil until the soil became saturated. This phase of the test lasted about 48 h without opening the outlet valve. Then it was opened and the amount of eroded soil was measured. After that, the settlement and final void ratio of the fine-grained layer were also calculated based on the method described by Premkumar et al. (2015). The working platform material was replaced for each test. The same procedure was followed for all tests with different curing time periods and percentages of nanosilica. Thus, by contact erosion test results, the effect of curing time, nanosilica addition, and dispersivity were investigated on contact erosion parameters. The results of contact erosion test performed on the untreated dispersive clay are given in Table 4.

3. Results and discussions

3.1. Effects of nanosilica treatment on the soil dispersivity

Fig. 5 shows the variations of soil dispersivity determined from double hydrometer tests for treatment periods of 1, 7, 14, and 28 days and different amounts of nanosilica used to stabilize the soil. It can be seen that the addition of nanosilica led to reduction of the dispersivity potential of

Table 4
Contact erosion test results carried out on dispersive clay sample.

Parameters	Quantity measured
Eroded soil extracted from the apparatus, gr	32.8
Eroded soil from the interface zone, gr	52.4
Cumulative eroded soil, gr	85.2
Initial dry weight, KN/m^3	17.2
Final dry weight, KN/m^3	16.826
Initial void ratio (e_0)	0.5245
Final void ratio (e_f)	0.5584
Initial soil particle volume (V_{sin}), m^3	0.01467
Final soil particle volume (V_{sf}), m^3	0.01435
Initial soil pore volume (V_{vin}), m^3	0.00769
Final soil pore volume (V_{vf}), m^3	0.008013
Settlement (S), mm	6.99

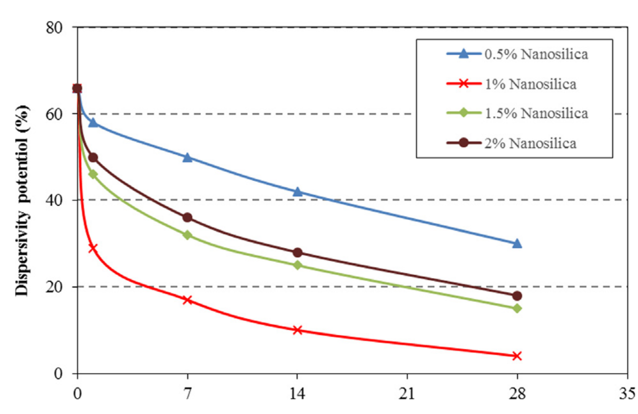

Fig. 5. Variations in dispersivity potential of nanosilica-stabilized dispersive soil for up to 28 days of curing.

the samples. Adding 1% nanosilica, the dispersivity potential reduced by about 56% after only 1 day of treatment, whereas in treatment with 0.5% nanosilica, this value was reached after 28 days. By increasing the curing time from 1 to 28 days, the sample containing 1% nanosilica reached the lowest dispersion which decreased by 93%, it means dispersion became 4%. According to Table 2, the soil used in this study contains large amounts of calcium compounds. Application of nanosilica in high treatment period causes SiO_2 particles to react with Ca^{2+} and form calcium silicate hydrate (CSH) gel. This gel also improves the dispersivity of the specimens. Nanoparticles of silica show high pozzolanic activity caused by high amounts of pure amorphous SiO_2 (Bahmani et al., 2014). With proper treatment time and reactions completion, the behaviour of the high plasticity soil changes to low plasticity soil (Kalkan, 2009). As shown in Table 5, the qualitative dispersivity of all samples was also assessed using pinhole test. As it is clear from the results, adding 0.5% nanosilica had little effect on soil dispersivity, whereas 1% nanosilica caused the dispersive soil to be stabilized even after the first day of treatment. The addition of further nanosilica up to 2% resulted in an adverse effect on the dispersibility corresponding to dispersion problems. The increase of nanosilica contents beyond the optimum value in the soil sample leads to the increased number of nanoparticles in the volume unit due to the lack of their homogeneous distribution (Bahmani et al., 2014). This is associated with the presence of weak lumps in the samples causing the negative effects on soil characteristics. According to the results of double hydrometer and pinhole tests, the curing time has a positive effect on the stabilization of dispersive soil, such that increasing the curing time reduces the soil dispersivity.

As stated by many researchers (Arora et al., 2019; Ghasabkolaei et al., 2017), if nanosilica is added to soils that do not contain Ca^{2+}, it will not affect their engineering behavior. While in the case of soils containing high amounts of Ca^{2+}, nanosilica can participate in the reactions and strengthen the bond between the particles. In this study, the use of nanosilica in high treatment period caused SiO_2 particles to react with Ca^{2+} and form calcium silicate hydrate (CSH) gel improving the dispersivity of the specimens.

Table 5
Classification of soils by pinhole test.

Test	Nanosilica, %	Curing time, day	Dispersive classification	Head
1	0	1	D2	50
2	0.5	1	D2	50
3	0.5	7	D2	50
4	0.5	14	ND3	180
5	0.5	28	ND2	1020
6	1	1	ND2	1020
7	1	7	ND1	1020
8	1	14	ND1	1020
9	1	28	ND1	1020
10	1.5	1	ND4	50
11	1.5	7	ND3	380
12	1.5	14	ND2	1020
13	1.5	28	ND1	1020
14	2	1	ND4	50
15	2	7	ND3	180
16	2	14	ND2	1020
17	2	28	ND1	1020

3.2. *Effect of nanosilica on the characteristics of contact erosion*

In the contact erosion test, the particles of the base clay were separated from each other and moved in water by the penetration of water through the fine-grained layer. These particles were floated in water and each of them was disintegrated into smaller ones and moved downward in the testing mould. Some of these particles were clogged in the coarse grains, and some others crossed the coarse layer and were accumulated at the bottom of the testing mould in the conical container. In general, the amount of eroded soil increased with increasing the time of soil–water contact. However, the amount of soil clogged in the coarse-grained layer was greater than the discharged soil from the apparatus. This could be due to either the type of soil (that means the influential features like plasticity or adhesion) or the low water pressure (not high enough to make the particles pass through the coarse-grained layer when the outlet valve was open). Figs. 6 and 7 illustrate the changes in contact erosion parameters, i.e. collected eroded soil mass and settlement of the nanosilica-stabilized dispersive soil, respectively, for up to 28 days of treatment. According to the results, the highest collected eroded soil mass and settlement were measured for the untreated soil, equal to 85.2 g and 6.99 mm, respectively. The bond between the dispersive soil particles becomes very weak when they are in contact with water and the consequent separation of these particles from one another causes the formation of cavities inside the soil, which leads to the settlement. It can be seen that the lowest quantities of collected eroded soil mass and settlement were achieved by adding 1% nanosilica to the samples, such that their values

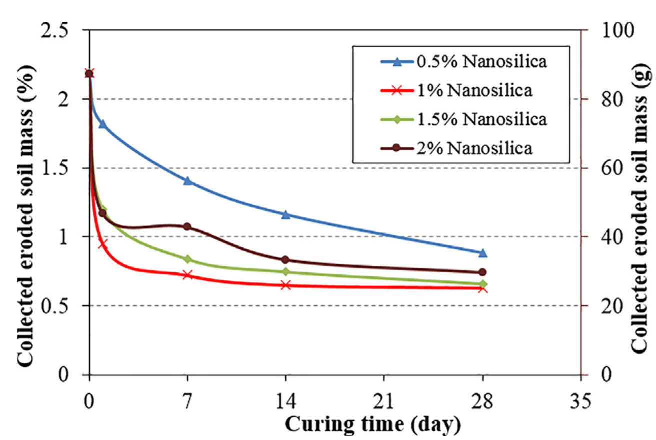

Fig. 6. Variations in collected eroded soil of nanosilica-stabilized dispersive soil for up to 28 days of curing.

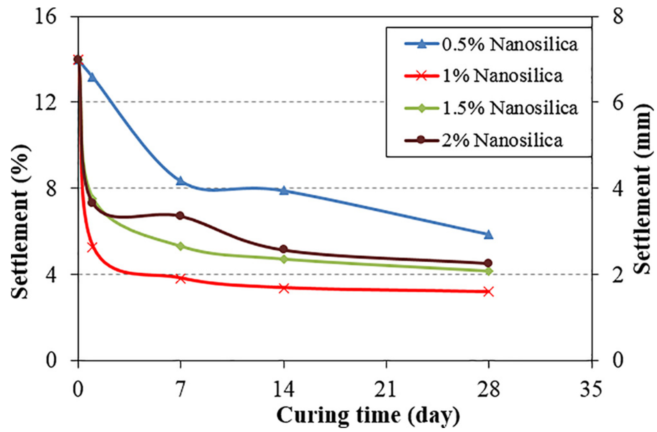

Fig. 7. Variations in settlement of nanosilica-stabilized dispersive soil for up to 28 days of curing.

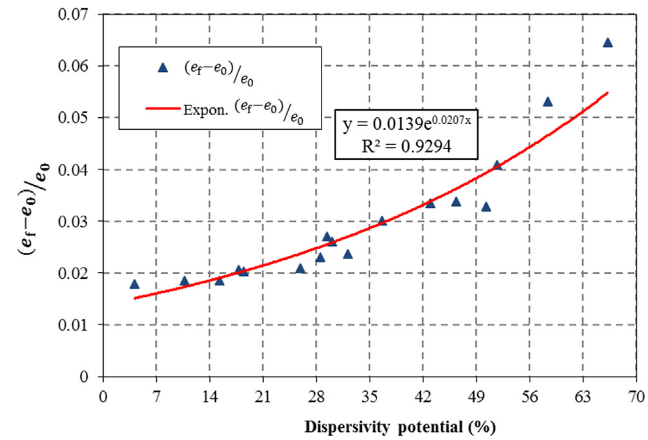

Fig. 8. Dispersivity potential of nanosilica-stabilized soil with respect to void ratio.

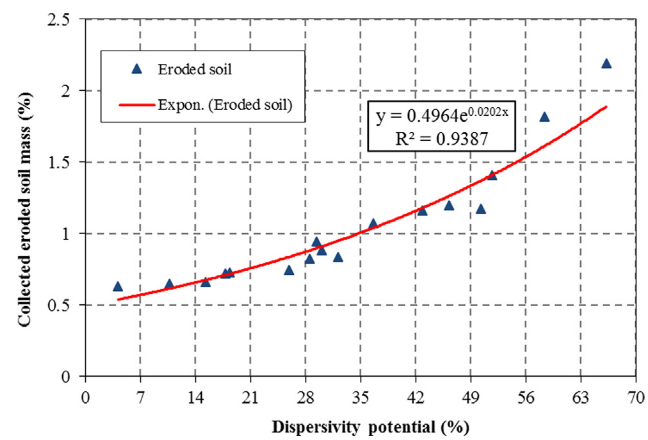

Fig. 9. Dispersivity potential of nanosilica-stabilized soil with respect to collected eroded soil mass.

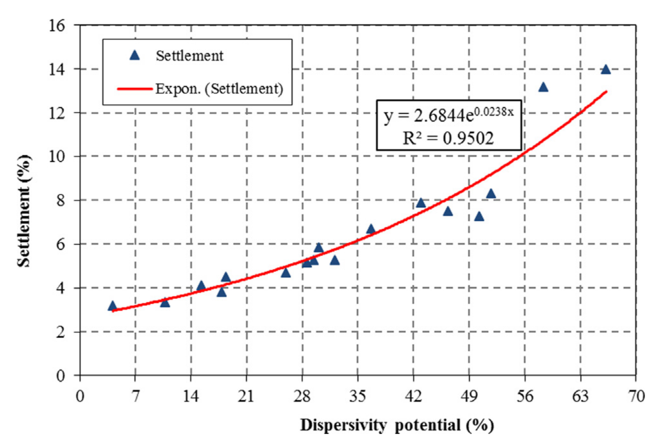

Fig. 10. Dispersivity potential of nanosilica-stabilized soil with respect to settlement.

after 7 days of treatment were 24.23 g and 1.58 mm, respectively, and they remained almost constant for longer period of treatment. This was due to the participation of the nanosilica in chemical reactions and consequently, the stronger bond between the particles of the soil –as the particles were less separated from each other and fewer cavities were created (Bahmani et al., 2016). Anyone could visually verify the validity of this claim considering the amount of clarity/transparency of the outlet water from the apparatus; which was more transparent for the stabilized soil in contrast to the test on the untreated soil.

3.3. Correlations between dispersivity and the characteristics of contact erosion

The establishment of appropriate correlations between various physical parameters based on the experimental results is of great importance, especially in geotechnical engineering. Excessive attempts have been made by researchers to find logical relationships between different geotechnical parameters (Sharma and Singh, 2018). In this regard, finding logical relationships among the results of the contact erosion test and other geotechnical properties of the soil can be of particular importance.

The contact erosion parameters were also estimated using the correlations between dispersivity potential and final void ratio, collected eroded soil mass, and settlement. Due to the lack of proper access to the contact erosion apparatus for all engineers, the use of these formulas can be helpful in predicting contact erosion parameters of dispersive soil under road pavement. In this study, the correlation between the dispersivity potential and each contact erosion parameter of the final void ratio, collected eroded soil mass, and settlement were investigated, as shown in Figs. 8, 9 and 10, respectively. For this purpose, the results of 17 contact erosion tests on dispersive and nanosilica-stabilized dispersive soil samples during 1, 7, 14 and 28 days of treatment were utilized. The regression lines were drawn through each set of data as exponential; which presented the highest R^2. In other words, as given in Table 6, the best-fit expressions in this case are governed by exponential functions of Eqs. (1)–(3). The value of R^2 can be interpreted as the ratio of variance in y-axis to the variance in x-axis. In the formulas presented in Table 5, the proximity

Table 6
Correlation formulas between contact erosion parameters and dispersivity potential.

Parameter	Formula	R^2
Void ratio and dispersivity potential	$\frac{(e_f - e_0)}{e_0} = 0.0139 \exp(0.0207D)$	0.9294
Collected eroded soil and dispersivity potential	$\frac{m}{m_0} = 0.4964 \exp(0.0202D)$	0.9387
Settlement and dispersivity potential	$\frac{S}{H} = 2.6844 \exp(0.0238D)$	0.9502

of this parameter to 1 means less deviation of the data from the correlation line, and finally shows the precision of the estimations.

$$\frac{(e_f - e_0)}{e_0} = 0.0139\ \exp(0.0207D) \tag{1}$$

$$\frac{m}{m_0} = 0.4964\ \exp(0.0202D) \tag{2}$$

$$\frac{S}{H} = 2.6844\ \exp(0.0238D) \tag{3}$$

where D is the soil dispersivity in percent, e_f and e_0 are the final and initial void ratios of soil, m and m_0 are the eroded and initial soil mass in mm, S and H are the soil settlement and the initial soil height in mm, respectively.

Using dimensionless parameters can eliminate dependent variables and make the graphs more concise. For this purpose, the void ratio, collected eroded soil mass, and settlement were presented as normalized ratios to eliminate their units. Therefore, the results can be generalized to dispersive soils with similar properties, such as the coefficient of uniformity and the average size of the particles. The effective application of non-dimensional parameters has also been proposed in previous studies (Arulrajah et al., 2016; Sultana and Dey, 2019). These equations are very useful because the contact erosion parameters, which are time consuming to be measured, can be almost precisely estimated only by knowing the soil dispersivity. The results show that there were strong correlations between dispersivity of the soil sample and its contact erosion parameters. In other words, the final void ratio, eroded soil mass, and settlement of the soil increased by increasing the soil dispersivity. It should be noted that these equations can be applied for dispersive soils with similar conditions and more research may investigate whether it can be utilized for a wider range of soils and conditions. The results obtained from the current study are in agreement with those published by Vakili et al. (2015a); in which by increasing the soil dispersivity, the internal erosion rate, segregation and deflocculation of the soil increased.

3.4. Effects of nanosilica treatment on the soil plasticity

The plasticity index (PI) is described as a criterion for determining the percentage of water content in which the soil is in a plastic state and characterizes the difference between the liquid limit (LL) and the plastic limit (PL). In other words, the PI value provides an approximate understanding of the behavior and properties of soils (Salimi et al., 2018). The effect of 0.5–2% nanosilica on the plasticity index of dispersive soil after 1, 7, 14, and 28 days of treatment is shown in Fig. 11. As can be understood from the figure, the plasticity index of all samples decreased with increasing curing time and the variations were more significant in the sample containing 1% nanosilica. This may be corresponded to short-term reactions, as well as a slight coating of nanosilica particles around the active surfaces of clay particles (Bahmani et al., 2014). The addition of 1% nanosilica to dispersive soil after 28 days of curing reduced PI from 23 to 14%. The quantity of PI increased for higher amounts of nanosilica, such that the PI of samples containing 1.5 and 2% nanosilica after 28-day treatment was equal to 16 and 17%, respectively. The PI reduction of the dispersive soil samples due to nanosilica addition can be considered as a beneficial change because the workability of the stabilized clay is improved.

3.5. Effects of nanosilica treatment on unconfined compressive strength (UCS)

The variations of unconfined compressive strength of nanosilica-stabilized dispersive soil after treatment periods of up to 28 days are shown in Fig. 12. Based on the results, the compressive strength increased by adding up to 1% nanosilica. Increasing the strength in the presence of nanosilica is due to the filling properties of its particles, which eliminates small soil pores. However, higher amount of nanosilica had an adverse effect on the samples and the compressive strength reduced. The reason is the occurrence of no reaction among soil and nanosilica ions, which may be correspondent to the limited movement of particles and their inadequate dispersion (Bahmani et al., 2014). Hence, the highest UCS was obtained when 1% nanosilica was added to the dispersive soil for all curing times.

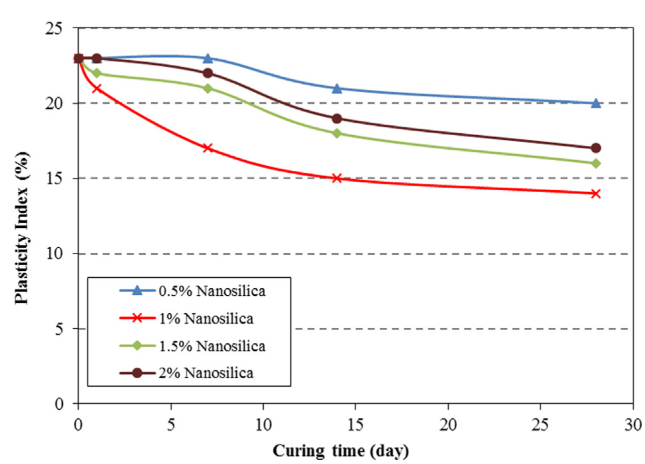

Fig. 11. Variation in plasticity index of nanosilica-treated dispersive clay for up to 28 days of curing.

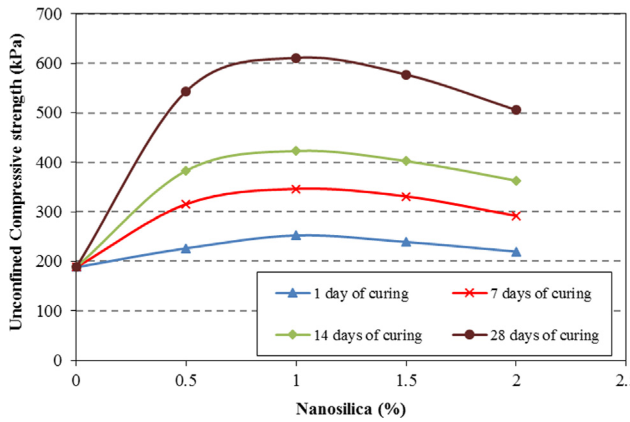

Fig. 12. Variation in UCS of nanosilica-treated dispersive clay for up to 28 days of curing.

On the other hand, increasing the curing time of samples stabilized with nanosilica also increased the compressive strength. By adding 1% nanosilica to the samples after 1 and 28 days of treatment, the UCS values were 252 and 611 kPa, respectively; which can be justified by completing long-term chemical reactions (Afrasiabian et al., 2019). Therefore, according to the results obtained in this study, the optimal percentage of nanosilica stabilizer for compressive strength has been 1% because it showed the best performance in short- and long-term unconfined compressive strength improvement. It should be noted that the optimum amount of 1% nanosilica is not general and can be used for the materials tested in this study.

3.6. Effects of nanosilica treatment on the soil microstructure

Fig. 13a, c, b, d and e show the scanning electron micrographs (SEM) of untreated, 1% nanosilica-treated and 2% nanosilica-treated samples, respectively, after 7 days of curing. The comparison of the figures reveals that the untreated soil particles have a dispersed structure and the number of pores among them is much higher than that of the treated soil. Moreover, the addition of only 1% nanosilica to the soil sample causes the particles to flocculate, and it decreases the number of these pores. It should be noted that most of these transformations to a flocculated structure are followed by short-term reactions such as cation exchange (Goodarzi and Salimi, 2015b). Adding nanosilica to soil leads to chemical reactions and denser soil matrix, filling the pores between the particles, and ultimately, the increase in the strength of the studied soil. As shown in Fig. 13e, the excess content of nanosilica beyond

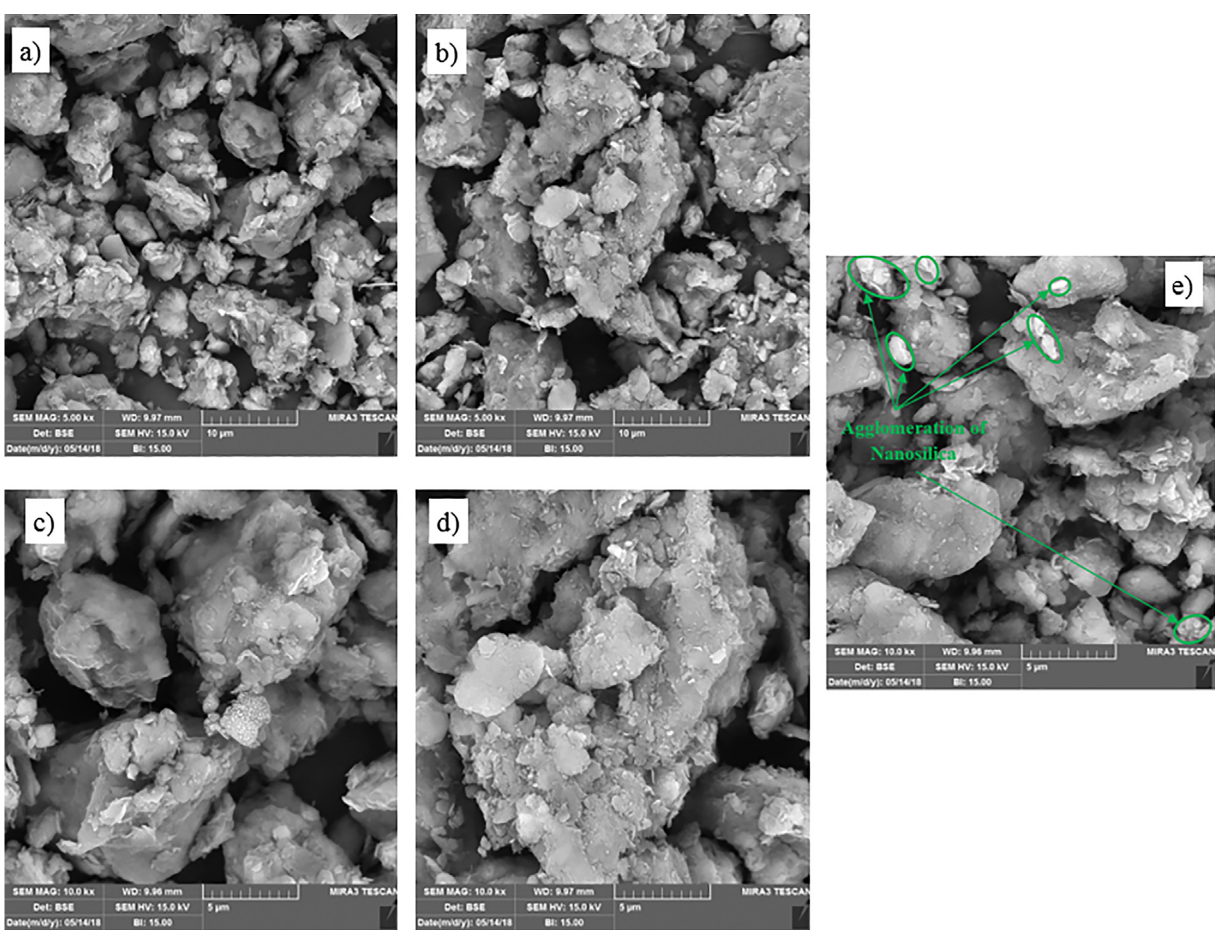

Fig. 13. SEM micrographs; (a, c) dispersive soil sample, (b, d) treated dispersive soil with 1% nanosilica and (e) treated dispersive soil with 2% nanosilica after 7 days of curing.

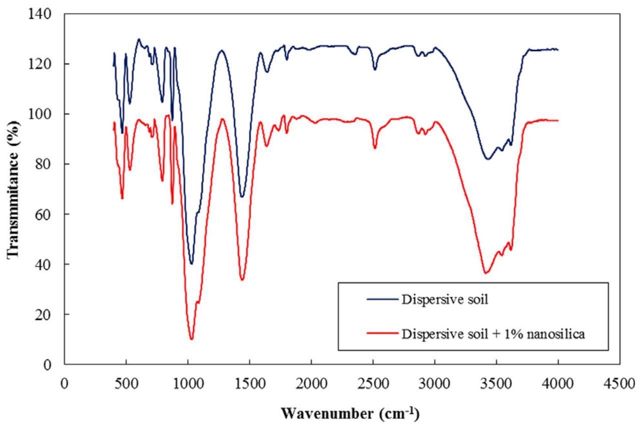

Fig. 14. FTIR spectra of untreated and 1% nanosilica-treated dispersive soil.

the optimum amount leads to the lack of their homogeneous distribution and to an agglomeration of nanosilica particles resulting the presence of weak lumps in the sample.

To understand better the interaction between the soil and nanosilica particles, the Fourier Transform Infrared (FTIR) spectra tests were carried out on the untreated and 1% nanosilica-treated soils, and their results are shown in Fig. 14. Both infrared spectra showed absorption bands at a nearly identical location. As can be seen, after treatment with nanosilica, the intensity of the bands at about 3410–3620 cm^{-1} increased compared to the dispersive clay, which are related to stretching vibration of surface hydroxyl groups. In addition, an increase in the intensity of bands at 792 cm^{-1} corresponds to the —OH bending vibration. These variations in the intensity of characteristic bands indicated that the chemical reactions occur between silica particles themselves, as well as between silica particles and hydroxyl groups of clay surfaces.

4. Conclusions

In this research, an apparatus was developed to study the nanosilica-stabilized dispersive soil behavior under the phenomenon of contact erosion in road construction. For this purpose, different amounts of nanosilica were added to the specimens and the geotechnical features were assessed after up to 28 days of treatment in the apparatus. The results provide a good approximation of the effect of nanosilica on contact erosion in dispersive soils with similar properties. The following conclusions can be summarized from the results of the experiments in this study:

- It was found that increasing the amount of nanosilica stabilizer up to 1% reduced dispersivity potential, the collected eroded soil mass, and settlement. Whereas an increase of more than 1% nanosilica had a negative effect on the mentioned parameters. Hence, the best value of nanosilica for the stabilization of dispersive soil in this study was 1%.
- Based on the results of double hydrometer and pinhole tests, the curing time of samples stabilized with nanosilica played a significant role in reducing soil dispersivity. As the curing time increased from 1 to 28 days in a sample containing 1% nanosilica, the dispersivity potential was significantly reduced by about 38%.
- The contact erosion parameters were estimated using the correlation relationships presented between dispersivity potential and final void ratio, the collected eroded soil mass, and settlement. Due to the lack of proper access to the contact erosion apparatus for all engineers, the use of these formulas can be helpful in predicting dispersive soil behavior under road pavement.
- The use of nanosilica can be an economically and environmentally appropriate option to stabilize the dispersive soils due to the low amount of it used as stabilizer. Addition of nanosilica and selecting an appropriate curing time improved the UCS of the samples. The UCS of samples treated by 1% nanosilica after 1 and 28 days of curing increased by 1.34 and 3.25 times, respectively, compared to the untreated one. Consequently, the treatment process followed in this study reduced the plasticity index of dispersive clay embankment and led to improving its workability. Finally, the potential use of nanosilica in improving dispersive clay embankments were validated through the results obtained from SEM and FTIR tests, where more flocculated structures obtained for the sample treated with nanosilica in comparison to the untreated one.

References

Afrasiabian, A., Salimi, M., Movahedrad, M., Vakili, A.H., 2019. Assessing the impact of GBFS on mechanical behaviour and microstructure of soft clay. Int. J. Geotech. Eng., 1–11

Arora, A., Singh, B., Kaur, P., 2019. Performance of Nano-particles in stabilization of soil: a comprehensive review. Mater. Today Proc. 17, 124–130.

Arulrajah, A., Mohammadinia, A., Phummiphan, I., Horpibulsuk, S., Samingthong, W., 2016. Stabilization of recycled demolition aggregates by geopolymers comprising calcium carbide residue, fly ash and slag precursors. Constr. Build. Mater. 114, 864–873.

Bahmani, S.H., Farzadnia, N., Asadi, A., Huat, B.B.K., 2016. The effect of size and replacement content of nanosilica on strength development of cement treated residual soil. Constr. Build. Mater. 118, 294–306.

Bahmani, S.H., Huat, B.B.K., Asadi, A., Farzadnia, N., 2014. Stabilization of residual soil using SiO2 nanoparticles and cement. Constr. Build. Mater. 64, 350–359.

Beguin, R., Philippe, P., Faure, Y.-H., 2012b. Pore-scale flow measurements at the interface between a sandy layer and a model porous medium: application to statistical modeling of contact erosion. J. Hydraul. Eng. 139, 1–11.

Bilodeau, J.-P., Dore, G., Pierre, P., 2007. Erosion susceptibility of granular pavement materials. Int. J. Pavem. Eng. 8, 55–66.

Consoli, N.C., Samaniego, R.A.Q., Villalba, N.M.K., 2016. Durability, strength, and stiffness of dispersive clay–lime blends. J. Mater. Civ. Eng. 28, 4016124.

Cyril, G., Yves-Henri, F., Rémi, B., Chia-Chun, H., 2009. Contact erosion at the interface between granular coarse soil and various base soils under tangential flow condition. J. Geotech. Geoenviron. Eng. 136, 741–750.

de OS, H., Carlos, J., 1991. Associations of distress and diagnosis of bitumen-surfaced road pavements. Transp. Res. Rec.

Ghasabkolaei, N., Choobbasti, A.J., Roshan, N., Ghasemi, S.E., 2017. Geotechnical properties of the soils modified with nanomaterials: A comprehensive review. Arch. Civ. Mech. Eng. 17, 639–650.

Goodarzi, A.R., Salimi, M., 2015a. Stabilization treatment of a dispersive clayey soil using granulated blast furnace slag and basic oxygen furnace slag. Appl. Clay Sci. 108, 61–69.

Goodarzi, A.R., Salimi, M., 2015b. Effect of iron industry slags on the geotechnical properties and mineralogy characteristics of expansive clayey soils. Modares J. Civ. Eng. 15, 161–203.

Huang, Y.H., 2004. Pavement Analysis and Design. Pearson Prentice Hall, Up Saddle River, New Jersey.

Jegatheesan, P., Premkumar, S., Arulrajah, A., Disfani, M.M., Rajeev, P., 2015. Laboratory model test on contact erosion of dispersive soil beneath pavement layers. Geotech. Test. J. 38, 906–914.

Kalkan, E., 2009. Influence of silica fume on the desiccation cracks of compacted clayey soils. Appl. Clay Sci. 43, 296–302. https://doi.org/10.1016/j.clay.2008.09.002.

Kazmee, H., Tutumluer, E., Beshears, S., 2016. Pavement working platforms constructed with large-size unconventional aggregates. Transp. Res. Rec. 2578, 1–11.

Lv, Q., Chang, C., Zhao, B., Ma, B., 2018. Loess Soil Stabilization by Means of SiO 2 Nanoparticles. Soil Mech. Found. Eng. 54, 409–413.

Premkumar, S., 2017. Study of Contact Erosion Failure on Pavement Embankment with Dispersive Soil.

Premkumar, S., Piratheepan, J., Arulrajah, A., Disfani, M.M., Rajeev, P., 2015. Experimental study on contact erosion failure in pavement embankment with dispersive clay. J. Mater. Civ. Eng. 28, 04015179. https://doi.org/10.1061/(asce)mt.1943-5533.0001452.

Premkumar, S., Piratheepan, J., Arulrajah, A., Disfani, M.M., Rajeev, P., 2014. Deformation of pavement structure due to contact erosion failure below the pavement layers. In: 8th Australasian Congress on Applied Mechanics: ACAM 8. Engineers Australia, pp. 401.

Said, A.M., Zeidan, M.S., Bassuoni, M.T., Tian, Y., 2012. Properties of concrete incorporating nano-silica. Constr. Build. Mater. 36, 838–844.

Salimi, M., Ilkhani, M., Vakili, A.H., 2018. Stabilization treatment of Na-montmorillonite with binary mixtures of lime and steelmaking slag. Int. J. Geotech. Eng., 1–7 https://doi.org/10.1080/19386362.2018.1439294.

Savaş, H., Türköz, M., Seyrek, E., Ünver, E., 2018. Comparison of the effect of using class C and F fly ash on the stabilization of dispersive soils. Arab. J. Geosci. 11, 612.

Schaefer, V.R., White, D.J., Ceylan, H., Stevens, L.J., 2008. Design guide for improved quality of roadway subgrades and subbases.

Sharma, L.K., Singh, T.N., 2018. Regression-based models for the prediction of unconfined compressive strength of artificially structured soil. Eng. Comput. 34, 175–186.

Shoghi, H., Ghazavi, M., Kazemian, S., Moayedi, H., 2013. A state of art review of dispersive soils: identification methods perspective. Eur. J. Sci. Res. 107, 322–328.

Sultana, P., Dey, A.K., 2019. Estimation of ultimate bearing capacity of footings on soft clay from plate load test data considering variability. Indian Geotech. J. 49, 170–183.

Trani, L.D.O., Indraratna, B., 2010. Assessment of subballast filtration under cyclic loading. J. Geotech. Geoenviron. Eng. 136, 1519–1528.

Vakili, A.H., Bin Selamat, M.R., Abdul Aziz, H.Bin, 2015a. Filtration of broadly graded cohesive dispersive base soils. J. Geotech. Geoenviron. Eng. 141, 04015004. https://doi.org/10.1061/(asce)gt.1943-5606.0001280.

Vakili, A.H., Bin Selamat, M.R., Mohajeri, P., 2016. Discussion of "Experimental Study on Contact Erosion Failure in Pavement Embankment with Dispersive Clay" by S. Premkumar, J. Piratheepan, A. Arulrajah, M. Disfani, and P. Rajeev. J. Mater. Civ. Eng. 29, 07016003. https://doi.org/10.1061/(asce)mt.1943-5533.0001452.

Vakili, A.H., Davoodi, S., Arab, A., Selamat, M.R., 2015b. Use of artificial neural network in predicting permeability of dispersive clay treated with lime and pozzolan. Ijsres 3, 23–37.

Vakili, A.H., Ghasemi, J.bin, Selamat, M.R., Salimi, M., Farhadi, M.S., 2018a. Internal erosional behaviour of dispersive clay stabilized with lignosulfonate and reinforced with polypropylene fiber. Constr. Build. Mater. 193, 405–415. https://doi.org/10.1016/j.conbuildmat.2018.10.213.

Vakili, A.H., Kaedi, M., Mokhberi, M., Selamat, M.R.B., Salimi, M., 2018b. Treatment of highly dispersive clay by lignosulfonate addition and electroosmosis application. Appl. Clay Sci. 152. https://doi.org/10.1016/j.clay.2017.11.039.

Vakili, A.H., Selamat, M.R.bin, Aziz, H.B.A., Mojiri, A., Ahmad, Z., Safarzadeh, M., 2017. Treatment of dispersive clay soil by ZELIAC. Geoderma 285, 270–279. https://doi.org/10.1016/j.geoderma.2016.10.009.

Vakili, A.H., Selamat, M.R. Bin, Mohajeri, P., Moayedi, H., 2018c. A critical review on filter design criteria for dispersive base soils. Geotech. Geol. Eng. 1–19. https://doi.org/10.1007/s10706-018-0453-7.

Vakili, A.H., Selamat, M.R., Moayedi, H., 2013. Effects of using Pozzolan and Portland cement in the treatment of dispersive clay. Sci. World J. 2013, 1–10. https://doi.org/10.1155/2013/547615.